Model-independent constraints on dark energy density from flux-averaging analysis of type IA supernovae data

Article (Published Version)

The Astrophysical Journal, 606:654–663, 2004 May 10

MODEL-INDEPENDENT CONSTRAINTS ON DARK ENERGY DENSITY FROM FLUX-AVERAGING ANALYSIS OF TYPE Ia SUPERNOVA DATA

Yun Wang[1] and Pia Mukherjee[1]
Received 2003 December 8; accepted 2004 January 27

ABSTRACT

We reconstruct the dark energy density $\rho_X(z)$ as a free function from current Type Ia supernova (SN Ia) data, together with the cosmic microwave background (CMB) shift parameter from CMB data from the *Wilkinson Microwave Anisotropy Probe* (*WMAP*), Cosmic Background Imager (CBI), and Arcminute Cosmology Bolometer Array Receiver (ACBAR), and the large-scale structure (LSS) growth factor from the Two-Degree Field (2dF) galaxy survey data. We parameterize $\rho_X(z)$ as a continuous function, given by interpolating its amplitudes at equally spaced z-values in the redshift range covered by SN Ia data, and a constant at larger z [where $\rho_X(z)$ is only weakly constrained by CMB data]. We assume a flat universe and use the Markov Chain Monte Carlo (MCMC) technique in our analysis. We find that the dark energy density $\rho_X(z)$ is constant for $0 \lesssim z \lesssim 0.5$ and increases with redshift z for $0.5 \lesssim z \lesssim 1$ at a 68.3% confidence level, but is consistent with a constant at a 95% confidence level. For comparison, we also give constraints on a constant equation of state for the dark energy. Flux averaging of SN Ia data is required to yield cosmological parameter constraints that are free of the bias induced by weak gravitational lensing. We set up a consistent framework for flux-averaging analysis of SN Ia data, based on the work of Wang. We find that flux averaging of SN Ia data leads to slightly lower Ω_m and smaller time variation in $\rho_X(z)$. This suggests that a significant increase in the number of SNe Ia from deep SN surveys on a dedicated telescope is needed to place a robust constraint on the time dependence of the dark energy density.

Subject headings: cosmology: observations — cosmological parameters — supernovae: general

1. INTRODUCTION

Observational data of Type Ia supernovae (SNe Ia) indicate that our universe is dominated by dark energy today (Riess et al. 1998; Perlmutter et al. 1999). The nature of dark energy is one of the great mysteries in cosmology at present. The time dependence of the dark energy density $\rho_X(z)$ can illuminate the nature of dark energy and help differentiate among the various dark energy models (for example, Freese et al. 1987; Peebles & Ratra 1988; Frieman et al. 1995; Caldwell, Dave, & Steinhardt 1998; Dodelson, Kaplinghat, & Stewart 2000; Deffayet 2001; Albrecht et al. 2002; Boyle, Caldwell, & Kamionkowski 2002; Freese & Lewis 2002; Griest 2002; Sahni & Shtanov 2003; Carroll, Hoffman, & Trodden 2003; Farrar & Peebles 2003; see Padmanabhan 2003 and Peebles & Ratra 2003 for reviews with more complete lists of references).

SNe Ia can be calibrated to be good cosmological standard candles, with small dispersions in their peak luminosity (Phillips 1993; Riess, Press, & Kirshner 1995). The measurements of the distance-redshift relations of SNe Ia are most promising for constraining the time variation of the dark energy density $\rho_X(z)$. The luminosity distance $d_L(z) = (1+z)\,r(z)$, with the comoving distance $r(z)$ given by

$$r(z) = cH_0^{-1} \int_0^z \frac{dz'}{E(z')} \tag{1}$$

for a flat universe, where

$$E(z) \equiv \left[\Omega_m(1+z)^3 + \Omega_k(1+z)^2 + \Omega_X \rho_X(z)/\rho_X(0)\right]^{1/2}, \tag{2}$$

with $\Omega_k \equiv 1 - \Omega_m - \Omega_X$. If the dark energy equation of state $w_X(z) = w_0 + w_1 z$, then

$$\frac{\rho_X(z)}{\rho_X(0)} = e^{3w_1 z}(1+z)^{3(1+w_0-w_1)}. \tag{3}$$

The dark energy density $\rho_X(z) = \rho_X(0)(1+z)^{3(1+w_0)}$ if the dark energy equation of state is a constant given by w_0.

Most researchers have chosen to study dark energy by constraining the dark energy equation of state w_X. However, because of the smearing effect (Maor, Brustein, & Steinhardt 2001) arising from the multiple integrals relating $w_X(z)$ to the luminosity distance of SNe Ia, $d_L(z)$, it is extremely hard to constrain w_X using SN data without making specific assumptions about w_X (Barger & Marfatia 2001; Huterer & Turner 2001; Maor et al. 2002; Wasserman 2002). If we constrain the dark energy density $\rho_X(z)$ instead, we minimize the smearing effect by removing one integral (Wang & Garnavich 2001; Tegmark 2002; Daly & Djorgovski 2003).

It is important that there are a number of other probes of dark energy that are complementary to SN Ia data (for example, see Podariu & Ratra 2001; Schulz & White 2001; Bean & Melchiorri 2002; Hu 2002; Sereno 2002; Bernstein & Jain 2004; Huterer & Ma 2003; Jimenez 2003; Majumdar & Mohr 2004; Mukherjee et al. 2003; Munshi & Wang 2003; Munshi, Porciani, & Wang 2004; Seo & Eisenstein 2003; Viel et al. 2003; Weller & Lewis 2003; Zhu & Fujimoto 2003). Since different methods differ in systematic uncertainties, the comparison of them allows for consistency checks, while the combination of them could yield tighter constraints on dark energy (for example, see Gerke & Efstathiou 2002; Hannestad & Mortsell 2002; Kujat et al. 2002).

The most pressing question about dark energy that can be addressed by observational data is whether the dark energy density varies with time. In order to constrain the time

[1] Department of Physics and Astronomy, University of Oklahoma, 440 West Brooks Street, Norman, OK 73019; wang@nhn.ou.edu, pia@nhn.ou.edu.

variation of dark energy density in a robust manner, it is important that we allow the dark energy density to be an arbitrary function of redshift z (Wang & Garnavich 2001; Wang & Lovelace 2001; Wang et al. 2003). In this paper, we present a model-independent reconstruction of the dark energy density $\rho_X(z)$, using SN Ia data published recently by the High-z Supernova Search Team (HZT) and the Supernova Cosmology Project (SCP) (Tonry et al. 2003; Barris et al. 2004; Knop et al. 2003), together with constraints from cosmic microwave background (CMB) data from the *Wilkinson Microwave Anisotropy Probe* (*WMAP*; Bennett et al. 2003), Cosmic Background Imager (CBI; Pearson et al. 2003), and Arcminute Cosmology Bolometer Array Receiver (ACBAR; Kuo et al. 2004), and large-scale structure (LSS) data from the Two-Degree Field (2dF) galaxy survey (Percival et al. 2002).

Note that for clarity of presentation, we label the samples of SNe Ia that we use according to the papers in which they were published. Hence we refer to the 194 SNe Ia from Tonry et al. (2003) and Barris et al. (2004) as the "Tonry/Barris sample" and the 58 SNe Ia from Knop et al. (2003) as the "Knop sample."

Flux averaging of SN Ia data is required to yield cosmological parameter constraints that are free of the bias induced by weak gravitational lensing (Wang 2000b). In this paper, we set up a consistent framework for flux-averaging analysis of SN Ia data, based on Wang (2000b).

We assume a flat universe, and use the Markov Chain Monte Carlo (MCMC) technique in our analysis.

Section 2 contains a consistent framework for flux-averaging analysis. We present our constraints on dark energy in § 3. A summary and discussion follow in § 4.

2. A CONSISTENT FRAMEWORK FOR FLUX-AVERAGING ANALYSIS

Since our universe is inhomogeneous in matter distribution, weak gravitational lensing by galaxies is one of the main systematics[2] in the use of SNe Ia as cosmological standard candles (Kantowski, Vaughan, & Branch 1995; Frieman 1997; Wambsganss et al. 1997; Holz & Wald 1998; Metcalf & Silk 1999; Wang 1999; Wang, Holz, & Munshi 2002; Munshi & Wang 2003). Flux averaging *justifies* the use of the distance-redshift relation for a smooth universe in the analysis of SN Ia data (Wang 2000b). Flux averaging of SN Ia data is required to yield cosmological parameter constraints that are free of the bias induced by weak gravitational lensing (Wang 2000b).[3] Here we set up a consistent framework for flux-averaging analysis of SN Ia data, based on Wang (2000b).

2.1. *Why Flux Averaging?*

The reason that flux averaging can remove or reduce gravitational-lensing bias is that because of flux conservation, the average magnification of a sufficient number of standard candles at the same redshift is 1.

The observed flux from a SN Ia can be written as

$$F(z) = F_{\rm int}\,\mu,$$
$$F_{\rm int} = F^{\rm tr}(z|\boldsymbol{s}^{\rm tr}) + \Delta F_{\rm int}, \tag{4}$$

where $F^{\rm tr}(z|\boldsymbol{s}^{\rm tr})$ is the predicted flux due to the true cosmological model parameterized by the set of cosmological parameters $\{\boldsymbol{s}^{\rm tr}\}$, $\Delta F_{\rm int}$ is the uncertainty in SN Ia peak brightness due to intrinsic variations in SN Ia peak luminosity and observational uncertainties, and μ is the magnification due to gravitational lensing by intervening matter. Therefore,

$$\Delta F^2 = \mu^2(\Delta F_{\rm int})^2 + (F_{\rm int})^2(\Delta\mu)^2. \tag{5}$$

Without flux averaging, we have

$$\begin{aligned}\chi^2_{N_{\rm data}}(\boldsymbol{s}^{\rm tr}) &= \sum_i \frac{\left[F(z_i) - F^{\rm tr}(z_i|\boldsymbol{s}^{\rm tr})\right]^2}{\sigma^2_{F,i}} \\ &= \sum_i \frac{\left[F^{\rm tr}(z_i)(\mu_i - 1)\right]^2 + \mu_i^2\left[\Delta F^{(i)}_{\rm int}\right]^2}{\sigma^2_{F,i}} \\ &\quad + 2\sum_i \frac{F^{\rm tr}(z_i)\Delta F^{(i)}_{\rm int}\,\mu_i(\mu_i - 1)}{\sigma^2_{F,i}} \\ &= N_{\rm data} + 2\sum_i \frac{F^{\rm tr}(z_i)\Delta F^{(i)}_{\rm int}\,\mu_i(\mu_i - 1)}{\sigma^2_{F,i}}.\end{aligned} \tag{6}$$

The flux averaging described in § 2.3 leads to the flux in each redshift bin

$$\overline{F}(\overline{z}_{i_{\rm bin}}) = F^{\rm tr}(\overline{z}_{i_{\rm bin}})\langle\mu\rangle_{i_{\rm bin}} + \langle\mu\Delta F_{\rm int}\rangle_{i_{\rm bin}}. \tag{7}$$

For a sufficiently large number of SNe Ia in the ith bin, $\langle\mu\rangle_{i_{\rm bin}} = 1$. Hence

$$\begin{aligned}\chi^2_{N_{\rm bin}}(\boldsymbol{s}^{\rm tr}) &\simeq \sum_{i_{\rm bin}}^{N_{\rm bin}} \frac{\left[\langle\mu\Delta F_{\rm int}\rangle_{i_{\rm bin}}\right]^2}{\sigma^2_{F,i_{\rm bin}}} \\ &\simeq \sum_{i_{\rm bin}}^{N_{\rm bin}} \frac{\left[\langle\Delta F_{\rm int}\rangle_{i_{\rm bin}}\right]^2}{\sigma^2_{F,i_{\rm bin}}} < N_{\rm bin}\end{aligned} \tag{8}$$

Comparison of equations (8) and (6) shows that flux averaging can remove or reduce the gravitational lensing effect and leads to a smaller χ^2 per degree of freedom for the true model, compared to that produced without flux averaging.

2.2. *Flux Statistics versus Magnitude Statistics*

Normally distributed measurement errors are required if the χ^2 parameter estimate is to be a maximum likelihood estimator (Press et al. 1994). Hence, it is important that we use the χ^2 statistics with an observable that has a error distribution closest to Gaussian.

So far, it has been assumed that the distribution of observed SN Ia peak brightness is Gaussian in *magnitudes*. Therefore, for a given set of cosmological parameters $\{\boldsymbol{s}\}$

$$\chi^2 = \sum_i \frac{\left[\mu_0(z_i) - \mu_0^p(z_i|\boldsymbol{s})\right]^2}{\sigma^2_{\mu_0}}, \tag{9}$$

where $\mu_0^p(z) = 5\log[d_L(z)/{\rm Mpc}] + 25$, and $d_L(z) = (1+z)r(z)$ is the luminosity distance.

However, while we do not have a very clear understanding of how the intrinsic dispersions in SN Ia peak luminosity are distributed, the distribution of observational uncertainties in SN Ia peak brightness is Gaussian in *flux*, since CCDs have replaced photometric plates as detectors of photons.

[2] The others systematics are possible gray dust (Aguirre 1999) and SN Ia peak luminosity evolution (Drell, Loredo, & Wasserman 2000; Riess et al. 1999; Wang 2000b); so far, there is no clear evidence of either.

[3] To avoid missing the faint end (which is fortunately steep) of the magnification distribution of observed SNe Ia, only SNe Ia detected well above the threshold should be used in flux averaging.

In this paper, we assume that the intrinsic dispersions in SN Ia peak brightness is Gaussian in *flux*, and not in magnitude as assumed in all previous publications. The justifications for this preference will be presented in detail elsewhere (Y. Wang et al. 2004, in preparation).[4] Thus,

$$\chi^2_{N_{\rm data}}(\boldsymbol{s}) = \sum_i \frac{[F(z_i) - F^p(z_i|\boldsymbol{s})]^2}{\sigma^2_{F,i}}. \quad (10)$$

Since the peak brightness of SNe Ia have been given in magnitudes with symmetric error bars, $m_{\rm peak} \pm \sigma_m$, we obtain equivalent errors in flux as follows:

$$\sigma_F \equiv \frac{F(m_{\rm peak} + \sigma_m) - F(m_{\rm peak} - \sigma_m)}{2}. \quad (11)$$

We will refer to equation (9) as "magnitude statistics" and equation (10) as "flux statistics." For reference and comparison, we present results in both magnitude statistics and flux statistics in this paper. However, a consistent framework for flux averaging is only straightforward in flux statistics.[5]

2.3. *A Recipe for Flux Averaging*

The procedure for flux averaging in Wang (2000b) is for minimizing χ^2 using the subroutines from Press et al. (1994). As described in Wang (2000b), the fluxes of SNe Ia in a redshift bin should only be averaged *after* removing their redshift dependence, which is a model-dependent process. For χ^2 statistics using MCMC or a grid of parameters, here are the steps in flux averaging:

1. Convert the distance modulus of SNe Ia into "fluxes,"

$$F(z_j) \equiv 10^{-[\mu_0(z_j)-25]/2.5} = \left[\frac{d_L^{\rm data}(z)}{\rm Mpc}\right]^{-2}. \quad (12)$$

2. For a given set of cosmological parameters $\{\boldsymbol{s}\}$, obtain "absolute luminosities" $\{\mathcal{L}(z_j)\}$ by removing the redshift dependence of the fluxes, i.e.,

$$\mathcal{L}(z_j) \equiv d_L^2(z_j|\boldsymbol{s})F(z_j). \quad (13)$$

3. Flux average the "absolute luminosities" $\{\mathcal{L}^i_j\}$ in each redshift bin i to obtain $\overline{\mathcal{L}}^i$:

$$\overline{\mathcal{L}}^i = \frac{1}{N}\sum_{j=1}^{N} \mathcal{L}^i_j(z^i_j),$$

$$\overline{z}_i = \frac{1}{N}\sum_{j=1}^{N} z^i_j, \quad (14)$$

4. Place $\overline{\mathcal{L}}^i$ at the mean redshift $\overline{z}_i$ of the ith redshift bin, and now the binned flux is

$$\overline{F}(\overline{z}_i) = \overline{\mathcal{L}}^i / d_L^2(\overline{z}_i|\boldsymbol{s}) \quad (15)$$

The 1 σ error on each binned data point $\overline{F}^i$, σ^F_i, is taken to be the rms of the 1 σ errors on the unbinned data points in the ith redshift bin, $\{F^i_j\}$ ($j = 1, 2, \ldots, N$), multiplied by $1/N^{1/2}$ (see Wang 2000a).

5. For the flux-averaged data, $\overline{F}(\overline{z}_i)$, we find

$$\chi^2 = \sum_i \frac{[\overline{F}(\overline{z}_i) - F^p(\overline{z}_i|\boldsymbol{s})]^2}{\sigma^2_{F,i}}, \quad (16)$$

where $F^p(\overline{z}_i|\boldsymbol{s}) = [d_L(z|\boldsymbol{s})/{\rm Mpc}]^{-2}$.

3. CONSTRAINTS ON DARK ENERGY

The Tonry/Barris SN Ia sample consists of 194 SNe Ia with $z > 0.01$ and extinction $A_V < 0.5$ (Tonry et al. 2003; Barris et al. 2004). To examine the effect of the two SNe Ia at the high-redshift end ($z = 1.199$ and $z = 1.755$, respectively), we also present the results for 193 SNe Ia (omitting the SN Ia at $z = 1.755$) and 192 SNe Ia (omitting the two SNe Ia at $z = 1.199$ and $z = 1.755$).

The Knop SN Ia sample consists of 58 SNe Ia (the "All SCP SNe" data set from Knop et al. 2003). These data should be compared with $m_B^{\rm eff} = 5\log(H_0 d_L) + {\rm offset}$, with

$${\rm offset} = 5\log(2997.9/h) + 25 + M_{\rm SN}, \quad (17)$$

where $M_{\rm SN}$ is the peak absolute magnitude of SNe Ia. Note that for the Knop sample, the flux statistics must be done with a revised definition of flux,

$$F(z) = \left(\frac{[H_0 d_L(z)]^{\rm data}}{\rm Mpc}\right)^{-2} = 10^{-2\left(m_{\rm eff}^B - {\rm offset}\right)/5}, \quad (18)$$

to be compared with the theoretical prediction of $F^p(z|\boldsymbol{s}) = [H_0 d_L(z|\boldsymbol{s})/{\rm Mpc}]^{-2}$ for a given set of cosmological parameters $\{\boldsymbol{s}\}$.

Note that an additional uncertainty from the redshift dispersion due to peculiar velocity must be added to the uncertainty of each SN Ia data point. The Knop sample already includes a dispersion of 300 km s^{-1} along the line of sight. To add 500 km s^{-1} dispersion in z to the SN data in the Tonry/Barris sample, one must propagate $\sigma_z = c^{-1}500$ km s^{-1} into an additional uncertainty in the luminosity distance $d_L(z)$, then add it in quadrature to the published uncertainty in $d_L(z)$. Note that this process is *dependent* on the cosmological model and must be done for each set of cosmological parameters during the likelihood analysis (Riess et al. 1998; Wang 2000b).

To obtain tighter constraints on dark energy, we also include constraints from CMB and LSS in our analysis. Since CMB data clearly indicate that we live in a flat universe, we assume $\Omega_m + \Omega_X = 1$ in all our results.[6]

We use the MCMC technique,[7] illustrated for example in Lewis & Bridle (2002), in the likelihood analysis. At its best, the MCMC method scales approximately linearly in computation time with the number of parameters. The method samples from the full posterior distribution of the parameters, and from these samples the marginalized posterior distributions of the parameters can be estimated. We have derived

[4] Our study of intrinsic peak luminosities of nearby SNe Ia shows that their distribution is much more Gaussian in flux than in magnitude.

[5] If the dispersions in SN Ia peak brightness were Gaussian in magnitude, flux averaging would introduce a small bias.

[6] Allowing both Ω_m and Ω_X to vary would lead to greatly increased uncertainty in dark energy constraints, such that no interesting constraints could be obtained from current data.

[7] For a review, see R. M. Neal's paper available via anonymous ftp at ftp://ftp.cs.utoronto.ca/pub in the file /radford/review.ps.gz.

all our probability distribution functions (PDFs) of the cosmological parameters from 10^6 MCMC samples.

3.1. *The Likelihood Analysis*

We use a χ^2 statistic

$$\chi^2 = \chi^2_{\rm SN} + \chi^2_{\rm CMB} + \chi^2_{\rm LSS}, \tag{19}$$

where $\chi^2_{\rm SN}$ is given by equations (16) and (10) for flux statistics (with and without flux averaging), and equation (9) for magnitude statistics. $\chi^2_{\rm CMB}$ and $\chi^2_{\rm LSS}$ are contributions from CMB and LSS data, respectively. The likelihood $\mathcal{L} \propto e^{-\chi^2/2}$ if the measurement errors are Gaussian (Press et al. 1994).

When the cosmological parameters are varied, the shift in the whole CMB angular spectrum is determined by the shift parameter (Bond, Efstathiou, & Tegmark 1997; Melchiorri et al. 2003; Ödman at el. 2002)

$$\mathcal{R} = \sqrt{\Omega_m}\, H_0\, r(z_{\rm dec}), \tag{20}$$

where $r(z_{\rm dec})$ denotes the comoving distance to the decoupling surface in a flat universe. Note that this is a robust way to include CMB constraints since the CMB depends on Ω_m and h in the combination of the physical parameter $\Omega_m h^2$. The results from CMB data correspond to $\mathcal{R}_0 = 1.716 \pm 0.062$ (using results in Spergel et al. 2003). We include the CMB data in our analysis by adding $\chi^2_{\rm CMB} = [(\mathcal{R} - \mathcal{R}_0)/\sigma_{\mathcal{R}}]^2$, where $\mathcal{R}$ is computed for each model using equation (20).

Following Knop et al. (2003), we include the LSS constraints from 2dF in terms of the growth parameter $f = d\ln D/d\ln a$, where a is the cosmic scale factor, and D is the linear fluctuation growth factor $D(t) = \delta^{(1)}(\boldsymbol{x}, t)/\delta(\boldsymbol{x})$, given by

$$\ddot{D}(t) + 2H(z)\dot{D}(t) - \frac{3}{2}\Omega_m H_0^2 (1+z)^3 D(t) = 0, \tag{21}$$

where the dots denote derivatives with respect to t. The Hubble parameter $H(z) = H_0 E(z)$ (see eq. [2]). Since $\beta = f/b_1$, the 2dF constraints of $\beta(z \sim 0.15) = 0.49 \pm 0.09$ (Hawkins et al. 2003) and $b_1 = 1.04 \pm 0.11$ (Verde et al. 2002) yield $f_0 \equiv f(z = 0.15) = 0.51 \pm 0.11$. We include the 2dF constraints in our analysis by adding $\chi^2_{\rm LSS} = \left\{[f(z = 0.15) - f_0]/\sigma_{f_0}\right\}^2$, where $f = d\ln D/d\ln a$ is computed for each model using D obtained by numerically integrating equation (21).

Note that we have chosen to use only the most conservative and robust information, the CMB shift parameter and the LSS growth factor, from CMB and LSS observations.[8] It is important that the limits on these are independent of the assumption on dark energy made in the CMB and LSS data analysis. Furthermore, by limiting the amount of information that we use from CMB and LSS observations to complement the SN Ia data, we minimize the effect of the systematics inherent in the CMB and LSS data on our results.

3.2. *Constraints on a Constant Dark Energy Equation of State* w_0

The most popular and simplest assumption about dark energy is that it has a constant equation of state w_0. Here we present constraints on a constant dark energy equation of state.

Figure 1 shows the marginalized PDF of the matter density fraction Ω_m, the dimensionless Hubble constant h, and the constant dark energy equation of state w_0.

[8] These observations provide a vast amount of information as detailed in the publications from the *WMAP* and 2dF teams.

The first four rows of figures in Figure 1 are results obtained using the Tonry/Barris SN Ia sample, requiring that $z > 0.01$ and extinction $A_V < 0.5$ (which yields a total of 194 SNe Ia). To examine the effect of two SNe Ia at the high-redshift end ($z = 1.199$ and $z = 1.755$, respectively), we also present the results for 193 SNe Ia (omitting the SN Ia at $z = 1.755$) and 192 SNe Ia (omitting the two SNe Ia at $z = 1.199$ and $z = 1.755$). The solid, dotted, and dashed lines indicate the results for 192, 193, and 194 SNe Ia, respectively.

The first two rows of figures in Figure 1 are results for SN Ia data from the Tonry/Barris sample only, without (*first row*) and with (*second row*) flux averaging ($\Delta z = 0.05$). Note that inclusion of the two highest redshift SNe Ia at $z = 1.199$ and $z = 1.755$ leads to slightly higher Ω_m and more negative w_0. Flux averaging leads to a broader PDF for Ω_m, with somewhat lower mean Ω_m, and a broader PDF for h.

The third and fourth rows of figures in Figure 1 are results for SN Ia data from the Tonry/Barris sample, combined with constraints from CMB and LSS data. The inclusion of the two highest redshift SNe Ia at $z = 1.199$ and $z = 1.755$ makes less difference in the estimated parameters, since the inclusion of the CMB and LSS data reduces the relative weight of these two data points. The main effect of flux averaging is a broader PDF for h.

The fifth row of figures in Figure 1 are results obtained using 58 SNe Ia from the Knop sample, using flux-averaged statistics (*solid lines*) and magnitude statistics (*dotted lines*), respectively. Note that flux averaging significantly broadens all the PDFs. The central figure is equivalent to a PDF in h (see eq. [17]). These are consistent with similar results derived using the SNe Ia from the Tonry/Barris sample (third row of figures in Fig. 1).

Table 1 gives the marginalized 68.3% and 95% confidence levels (CLs) of Ω_m, h, and w_0. These have been computed using 10^6 MCMC samples.

3.3. *Constraints on Dark Energy Density as a Free Function*

To place model-independent constraints on dark energy, we parameterize $\rho_X(z)$ as a continuous function, given by interpolating its amplitudes at equally spaced z-values in the redshift range covered by SN Ia data ($0 \le z \le z_{\rm max}$), and a constant at larger z [$z > z_{\rm max}$, where $\rho_X(z)$ is only weakly constrained by CMB data]. The values of the dimensionless dark energy density $f_i \equiv \rho(z_i)/\rho_X(0)$ ($i = 1, 2, \ldots, n_f$) are the independent variables to be estimated from data. We interpolate $\rho_X(z)$ using a polynomial of order n_f for $0 \le z \le z_{\rm max}$.

Since the present data cannot constrain $\rho_X(z)$ for $n_f > 2$, we present results for $n_f = 2$, i.e., with $\rho_X(z)$ parameterized by its values at $z = z_{\rm max}/2$, $z_{\rm max}$.

Figure 2 shows the marginalized PDF of the matter density fraction Ω_m (*first column*), the dimensionless Hubble constant h (*second column*), and dimensionless dark energy density at $z = z_{\rm max}/2$ and $z = z_{\rm max}$ (*third and fourth columns, respectively*), obtained using current SN Ia data (Tonry et al. 2003; Barris et al. 2004; Knop et al. 2003), flux averaged and combined with CMB and 2dF data. The first three rows of figures are results for 192, 193, and 194 SNe Ia from the Tonry/Barris sample, while the fourth row are results for 58 SNe Ia from the Knop sample. The dark energy density at $z = z_{\rm max}$ is not well constrained when the $z = 1.755$ SN Ia is included in the analysis; this is as expected since this extends $\rho_X(z)$ to $z_{\rm max} = 1.755$, with only one SN Ia at $z > 1.2$.

Note that when the estimated parameters are well constrained, flux averaging generally leads to slightly lower estimates of Ω_m and $\rho_X(z)$ (at $z = z_{\rm max}/2$ and $z = z_{\rm max}$).

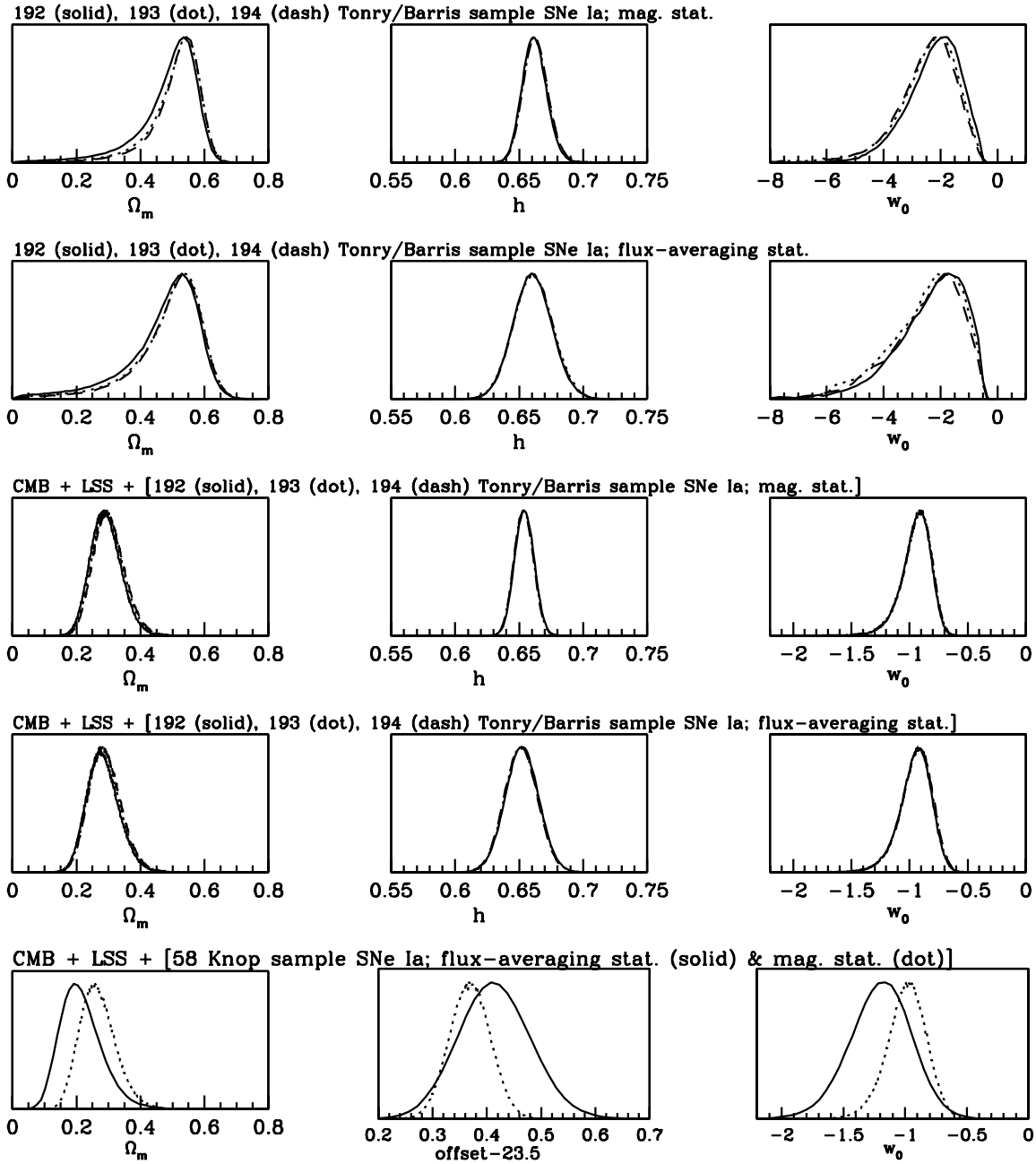

FIG. 1.—Marginalized probability distributions of Ω_m, h, and the constant equation of state for the dark energy w_0

Table 2 gives the marginalized 68.3% and 95% CLs of Ω_m, h, $\rho_X(z_{\max}/2)/\rho_X(0)$, and $\rho_X(z_{\max})/\rho_X(0)$. These have been computed using 10^6 MCMC samples.

Figure 3 shows the dark energy density $\rho_X(z)$ reconstructed from current SN Ia (the Tonry/Barris sample and the Knop sample), CMB, and LSS data. The heavy and light lines indicate the 68.3% and 95% CLs, respectively, of the reconstructed $\rho_X(z)$. The dot-dashed line indicates the cosmological constant model, $\rho_X(z)/\rho_X(0) = 1$. The 68.3% and 95% CLs of $\rho_X(z)$ are marginalized confidence levels, computed at each z using 10^6 MCMC samples, with the correlation between $\rho_X(0.5\,z_{\max})$ and $\rho_X(z_{\max})$ fully included.

Figure 3*a* shows the reconstructed $\rho_X(z)$ using 192, 193, and 194 SNe Ia from the Tonry/Barris sample, flux averaged and combined with CMB and LSS data. The densely and sparsely shaded regions are the 68.3% and 95% CLs, respectively, of $\rho_X(z)$ for 192 SNe Ia (at $z \leq 1.056$). The heavy and light lines are the 68.3% and 95% CLs, respectively, of $\rho_X(z)$ for 193 (*dotted lines*) and 194 SNe Ia (*dashed lines*). Note that the $\rho_X(z)$ reconstructed from 193 SNe Ia (adding the SN Ia at $z = 1.199$) nearly overlaps from that from 192 SNe Ia for $z \lesssim 1.056$. However, the $\rho_X(z)$ reconstructed from 194 SNe Ia (adding the SNe Ia at $z = 1.199$ and $z = 1.755$) deviates notably from that from 192 SNe Ia for $0.7 \lesssim z \lesssim 1.056$, although the 68.3% CL regions overlap. Clearly, the reconstructed $\rho_X(z)$ is constant for $0 \lesssim z \lesssim 0.5$ and increases with redshift z for $0.5 \lesssim z \lesssim 1$ at 68.3% CL but is consistent with a constant at 95% CL. We note that at 90% CL, $\rho_X(0.5z_{\max})/\rho(0) = [0.83, 1.59]$, and $\rho_X(z_{\max})/\rho(0) = [1.03, 6.85]$; this indicates that $\rho_X(z)$ varies with time at approximately 90% CL.

Figure 3*b* shows the reconstructed $\rho_X(z)$ using 192 SNe Ia from the Tonry/Barris sample (same as in Fig. 3*a*) and that

TABLE 1

ESTIMATED COSMOLOGICAL PARAMETERS ASSUMING $w_X(z) = w_0$

Type of Data	Ω_m	h[a]	w_0	$\chi^2_{\rm min}/N_{\rm dof}$[b]
Tonry/Barris Sample 192 SNe ($z_{\rm max} = 1.056$)				
Binned flux[c]	0.47, [0.36, 0.57], [0.14, 0.63]	0.661, [0.645, 0.674], [0.631, 0.690]	−2.37, [−3.56, −1.20], [−5.34, -0.69]	13.34/19
Unbinned flux	0.47, [0.43, 0.52], [0.34, 0.55]	0.656, [0.644, 0.666], [0.636, 0.676]	−3.08, [−4.09, −2.08], [−5.50, −1.46]	209.10/189
Unbinned magnitude	0.49, [0.41, 0.57], [0.22, 0.61]	0.662, [0.651, 0.671], [0.644, 0.681]	−2.25, [−3.18, −1.34], [−4.36, −0.80]	193.36/189
Tonry/Barris Sample 193 SNe ($z_{\rm max} = 1.199$)				
Binned flux[c]	0.48, [0.39, 0.58], [0.18, 0.63]	0.661, [0.645, 0.676], [0.631, 0.690]	−2.53, [−3.85, −1.30], [−5.54, −0.73]	14.36/20
Unbinned flux	0.48, [0.43, 0.52], [0.35, 0.56]	0.656, [0.645, 0.665], [0.637, 0.676]	−3.13, [−4.10, −2.13], [−5.64, −1.50]	210.56/190
Unbinned magnitude	0.51, [0.44, 0.58], [0.29, 0.62]	0.663, [0.653, 0.671], [0.644, 0.683]	−2.47 [−3.42, −1.49], [−5.14, −0.91]	194.86/190
Tonry/Barris Sample 194 SNe ($z_{\rm max} = 1.755$)				
Binned flux[c]	0.49, [0.40, 0.58], [0.20, 0.63]	0.661, [0.645, 0.675], [0.632, 0.690]	−2.54, [−3.80, −1.34], [−5.62, −0.76]	14.40/21
Unbinned flux	0.48, [0.44, 0.53], [0.37, 0.56]	0.656, [0.645, 0.665], [0.637, 0.675]	−3.17, [−4.13, −2.22], [−5.47, −1.58]	210.74/191
Unbinned magnitude	0.51, [0.45, 0.58], [0.30, 0.62]	0.663, [0.653, 0.671], [0.644, 0.683]	−2.51, [−3.46, −1.55], [−4.97, −0.95]	194.88/191
Tonry/Barris Sample 192 SNe ($z_{\rm max} = 1.056$) + CMB and LSS				
Binned flux[c]	0.28, [0.23, 0.33], [0.19, 0.39]	0.652, [0.638, 0.665], [0.627, 0.677]	−0.95, [−1.09, −0.82], [−1.27, −0.72]	15.44/21
Unbinned flux	0.26, [0.22, 0.31], [0.18, 0.36]	0.643, [0.634, 0.650], [0.627, 0.657]	−1.15, [−1.29, −1.00], [−1.53, −0.90]	216.76/191
Unbinned magnitude	0.29, [0.24, 0.34], [0.21, 0.39]	0.654, [0.646, 0.661], [0.639, 0.668]	−0.95, [−1.07, −0.83], [−1.24, −0.74]	196.60/191
Tonry/Barris Sample 193 SNe ($z_{\rm max} = 1.199$) + CMB and LSS				
Binned flux[c]	0.29, [0.24, 0.34], [0.20, 0.39]	0.652, [0.638, 0.663, [0.626, 0.676]	−0.95, [−1.08, −0.82] [−1.27, −0.71]	17.04/22
Unbinned flux	0.27, [0.22, 0.31], [0.18, 0.37]	0.643, [0.635, 0.650], [0.627, 0.658]	−1.15, [−1.29, −1.00], [−1.54, −0.90]	219.00/192
Unbinned magnitude	0.30, [0.25, 0.35], [0.21, 0.40]	0.654, [0.645, 0.660], [0.638, 0.667]	−0.95, [−1.07, −0.82], [−1.25, −0.74]	199.04/192
Tonry/Barris Sample 194 SNe ($z_{\rm max} = 1.755$) + CMB and LSS				
Binned flux[c]	0.29, [0.24, 0.34], [0.20, 0.40]	0.651, [0.638, 0.663], [0.625, 0.676]	−0.95, [−1.08, −0.81], [−1.28, −0.71]	17.44/23
Unbinned flux	0.27, [0.22, 0.32], [0.18, 0.37]	0.642, [0.634, 0.650], [0.627, 0.657]	−1.15, [−1.31, −1.00], [−1.57, −0.90]	219.8/193
Unbinned magnitude	0.30, [0.25, 0.35], [0.21, 0.41]	0.654, [0.645, 0.660], [0.638, 0.668]	−0.95, [−1.07, −0.82], [−1.27, −0.73]	199.50/193
58 Knop Sample SNe ($z_{\rm max} = 0.863$) + CMB and LSS				
Binned flux[c]	0.22, [0.15, 0.28], [0.11, 0.36]	0.414, [0.347, 0.480], [0.286, 0.547][d]	−1.20, [−1.45, −0.96], [−1.73, −0.74]	9.1/13
Unbinned flux	0.21, [0.16, 0.26], [0.13, 0.32]	0.395, [0.356, 0.434], [0.321, 0.471][d]	−1.18, [−1.34, −1.02], [−1.54, −0.88]	61.34/57
Unbinned magnitude	0.27, [0.21, 0.32], [0.17, 0.39]	0.367, [0.331, 0.406], [0.295, 0.441][d]	−0.99, [−1.15, −0.83], [−1.34, −0.70]	55.86/57

NOTE.—Parameters are given for the mean, 68.3%, and 95% confidence levels, respectively.

[a] Statistical error only, not including the contribution from the much larger SN Ia absolute magnitude error of $\sigma_h^{\rm int} \simeq 0.05$ (see § 4).

[b] The number of degrees of freedom.

[c] Flux averaged with $\Delta z = 0.05$.

[d] Offset −23.5.

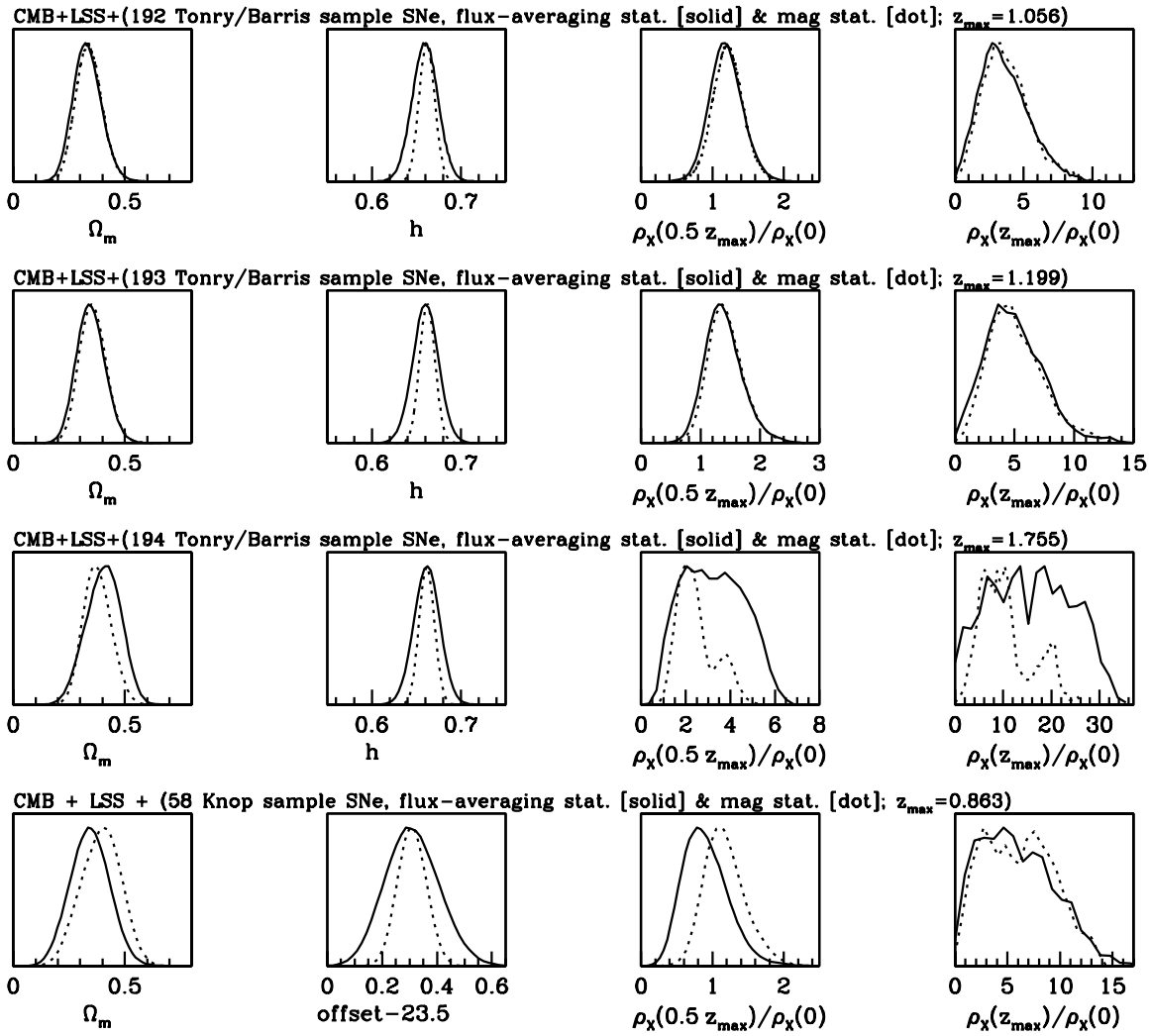

FIG. 2.—Marginalized probability distributions of Ω_m, h, and dimensionless dark energy density at $z = z_{\max}/2$ and $z = z_{\max}$

from the 58 SNe Ia of the Knop sample (*dotted lines*). The 68.3% CL regions overlap. However, the 58 SCP SNe Ia seem to favor $\rho_X(z) \lesssim 1$ at $0 \lesssim z \lesssim 0.5$ and has much larger uncertainties at $z \gtrsim 0.5$.

3.4. *Comparison with Previous Work*

The SN observational teams have published their data together with constraints on a constant dark energy equation of state (Tonry et al. 2003; Knop et al. 2003). These results should be compared with our results for a constant $w_X(z)$ using magnitude statistics (see Table 1). Using a 2dF prior of $\Omega_m h = 0.20 \pm 0.03$ (Percival et al. 2002) and assuming a flat universe, Tonry et al. (2003) found that $-1.48 < w_0 < -0.72$ at 95% CL; this is close to $-1.24 < w_0 < -0.74$ at 95% CL (using 192 SNe Ia together with CMB and LSS constraints as discussed in § 3.1) from Table 1. Using the same CMB and LSS constraints as us and assuming a flat universe, Knop et al. (2003) found that $w_0 = -1.05^{+0.15}_{-0.20}$ (statistical) ± 0.09 (identified systematics) at 68.3% CL: close to our results of $w_0 = -0.99 \pm 0.16$ at 68.3% CL.

At the completion of our analysis, we became aware that Alam et al. (2003) and Choudhury & Padmanabhan (2003) have found that current SN Ia data favor $w_X(z) < -1$. Although our results are qualitatively consistent with these, there are significant differences in both analysis technique and quantitative results.

Alam et al. (2003) used 172 SNe Ia from Tonry et al. (2003) and obtained a reconstructed $w_X(z)$ that deviates quite significantly from $w_X(z) = -1$. In their paper, Figures 3 and 14 (both assuming $\Omega_m = 0.3$) are consistent with our findings. We note that some of their reconstructed $w_X(z)$'s (see their Figs. 4, 6, 8, 10, and 16) have decreasing errors for $z \gtrsim 1.2$ (where there are only two SNe Ia). This illustrates the fact that while free-fitting forms for $\rho_X(z)$ or $w_X(z)$ generally give increasing errors with redshift (large error when there are very few observed SNe Ia; see Fig. 3 of this paper), this may not be true for other parameterizations (such as used in Alam et al. 2003).

Choudhury & Padmanabhan (2004) used 194 SNe Ia (the Tonry/Barris sample) and presented their results for $w_X(z) = w_0 + w_1 z/(1+z)$ with $\Omega_m = 0.29$, 0.34, and 0.39 (no marginalization over Ω_m).

4. SUMMARY AND DISCUSSION

In order to place model-independent constraints on dark energy, we have reconstructed the dark energy density $\rho_X(z)$ as a free function from current SN Ia data (Tonry et al. 2003; Barris et al. 2004; Knop et al. 2003), together with CMB and

TABLE 2

ESTIMATED COSMOLOGICAL PARAMETERS FOR ARBITRARY $\rho_X(z)$, FROM SN Ia DATA COMBINED WITH CMB AND LSS DATA

Type of Data	Ω_m	h[a]	$\rho_X(0.5z_{\max})/\rho_X(0)$	$\rho_X(z_{\max})/\rho_X(0)$	$\chi^2_{\min}/N_{\rm dof}$[b]
Tonry/Barris Sample 192 SNe ($z_{\max} = 1.056$)					
Binned flux[c]	0.33, [0.27, 0.39], [0.22, 0.46]	0.660, [0.644, 0.673], [0.630, 0.688]	1.19, [0.97, 1.42], [0.76, 1.67]	3.61, [0.84, 5.41], [0.73, 7.53]	13.28/20
Unbinned flux	0.34, [0.28, 0.39], [0.24, 0.45]	0.655, [0.645, 0.663], [0.637, 0.671]	1.09, [0.88, 1.31], [0.67, 1.56]	5.02, [3.27, 6.82], [1.98, 9.15]	208.26/190
Unbinned magnitude	0.34, [0.28, 0.40], [0.23, 0.46]	0.662, [0.652, 0.670], [0.645, 0.678]	1.22, [1.01, 1.43], [0.80, 1.66]	3.75, [2.05, 5.40], [0.94, 7.76]	193.30/190
Tonry/Barris Sample 193 SNe ($z_{\max} = 1.199$)					
Binned flux[c]	0.35, [0.28, 0.41], [0.23, 0.48]	0.660, [0.645, 0.674], [0.631, 0.688]	1.39, [1.08, 1.69], [0.84, 2.10]	4.95, [2.55, 7.34], [0.88, 10.35]	14.24/21
Unbinned flux	0.36, [0.30, 0.42], [0.25, 0.49]	0.656, [0.645, 0.664], [0.637, 0.672]	1.44, [1.06, 1.82], [0.80, 2.41]	7.50, [4.39, 10.69], [2.57, 15.57]	209.42/191
Unbinned magnitude	0.36, [0.30, 0.42], [0.25, 0.48]	0.662, [0.653, 0.670], [0.645, 0.678]	1.42, [1.13, 1.71], [0.89, 2.08]	5.14, [2.88, 7.43], [1.41, 10.62]	194.50/191
Tonry/Barris Sample 194 SNe ($z_{\max} = 1.755$)					
Binned flux[c]	0.40, [0.32, 0.48], [0.25, 0.54]	0.661, [0.646, 0.675], [0.632, 0.688]	3.26, [1.76, 4.76], [1.02, 5.75]	15.64, [6.22, 25.30], [0.92, 30.53]	14.5/22
Unbinned flux	0.38, [0.32, 0.43], [0.27, 0.48]	0.654, [0.644, 0.662], [0.637, 0.670]	2.85, [1.88, 3.81], [1.18, 4.69]	14.78, [[.77, 20.58], [4.36, 25.83]	209.88/192
Unbinned magnitude	0.38, [0.31, 0.44], [0.26, 0.50]	0.662, [0.652, 0.669], [0.645, 0.678]	2.48, [1.66, 3.54], [1.22, 4.35]	10.60, [5.41, 17.81], [2.68, 21.80]	194.70/192
Knop Sample 58 SNe ($z_{\max} = 0.863$)					
Binned flux[c]	0.34, [0.25, 0.43], [0.18, 0.52]	0.311, [0.210, 0.409], [0.127, 0.509][d]	0.91, [0.59, 1.22], [0.38, 1.61]	5.92, [2.13, 9.73], [0.58, 13.21]	7.2/12
Unbinned flux	0.26, [0.18, 0.33], [0.12, 0.41]	0.381, [0.331, 0.428], [0.286, 0.474][d]	0.85, [0.67, 1.03], [0.50, 1.21]	1.96, [0.53, 3.55], [0.09, 5.450]	61.32/56
Unbinned magnitude	0.39, [0.30 0.48], [0.22, 0.56]	0.309, [0.256, 0.362], [0.208, 0.412][d]	1.18, [0.89, 1.46], [0.67, 1.82]	6.10, [2.47, 9.59], [0.86, 12.57]	53.90/56

NOTE.—Parameters are given for the mean, 68.3%, and 95% confidence levels, respectively.

[a] Statistical error only, not including the contribution from the much larger SN Ia absolute magnitude error of $\sigma_h^{\rm int} \simeq 0.05$ (see § 4).

[b] The number of degrees of freedom.

[c] Flux averaged with $\Delta z = 0.05$.

[d] Offset -23.5.

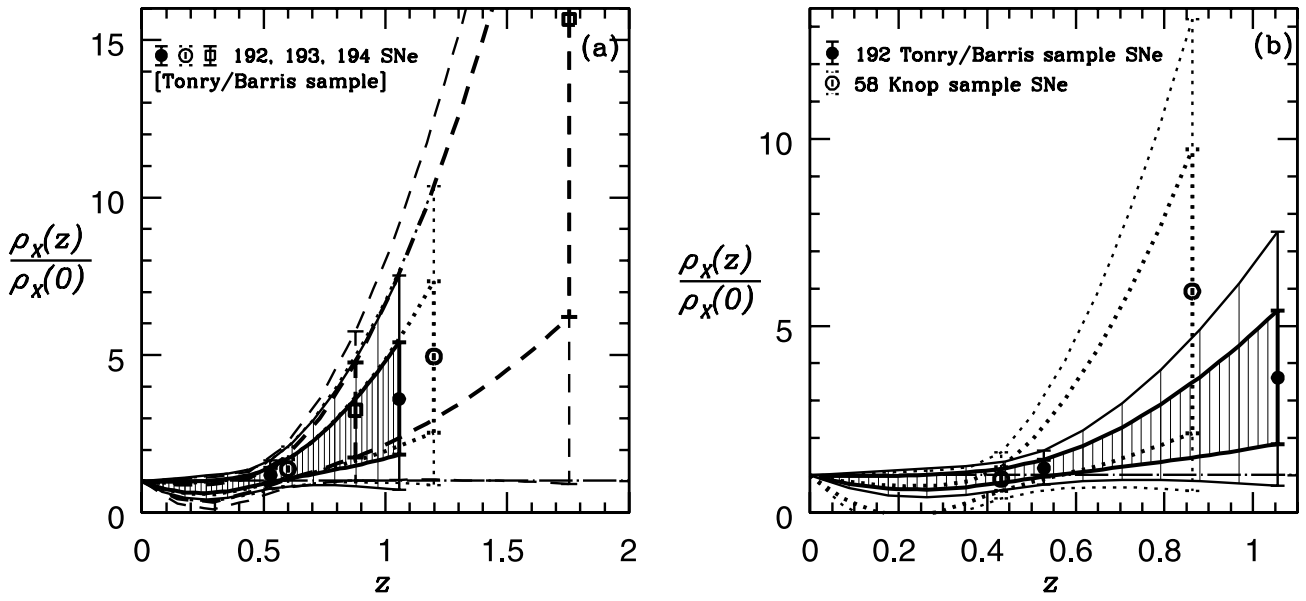

FIG. 3.—Dark energy density $\rho_X(z)$ reconstructed from current SN Ia (Tonry/Barris sample and Knop sample), CMB, and LSS data. The densely and sparsely shaded regions are the 68.3% and 95% CLs, respectively, of $\rho_X(z)$ for 192 Tonry/Barris sample SNe Ia (at $z \leq 1.056$). The heavy and light lines indicate the 68.3% and 95% CLs, respectively, of the reconstructed $\rho_X(z)$. The dot-dashed line indicates the cosmological constant model, $\rho_X(z)/\rho_X(0) = 1$. (*a*) Reconstructed $\rho_X(z)$ using 192 (*shaded regions*), 193 (*dotted lines*), and 194 (*dashed lines*) SNe Ia from the Tonry/Barris sample (Tonry et al. 2003; Barris et al. 2004). (*b*) Reconstructed $\rho_X(z)$ using 192 Tonry/Barris sample SNe Ia (*shaded regions*) and 58 Knop sample SNe Ia (*dotted lines*; Knop et al. 2003).

LSS data. We find that the dark energy density $\rho_X(z)$ is constant for $0 \lesssim z \lesssim 0.5$ and increases with redshift z for $0.5 \lesssim z \lesssim 1$ at 68.3% CL but is consistent with a constant at 95% CL (see Fig. 3).

Flux averaging of SN Ia data is required to yield cosmological parameter constraints that are free of the bias induced by weak gravitational lensing (Wang 2000b). We have developed a consistent framework for flux-averaging analysis of SN Ia data and applied it to current SN Ia data. We find that flux averaging of SN Ia data generally leads to slightly lower Ω_m and smaller time variation in $\rho_X(z)$.

We note that flux averaging of SNe Ia has more effect on the Knop sample than the Tonry/Barris sample. This may be due to the fact that the measurement errors of the majority of the SNe Ia in the Tonry/Barris sample have been "Gaussianized" in magnitude by averaging over several different analysis techniques (Tonry et al. 2003). However, it is likely that SN Ia peak brightness distribution is Gaussian in *flux*, instead of magnitude (Y. Wang et al. 2004, in preparation). A consistent framework for flux averaging is only straightforward (as presented in § 2) if the distribution of SN Ia peak brightnesses is Gaussian in flux. Our results suggest that observers should publish observed SN Ia peak brightnesses with uncertainties in flux, to allow detailed flux-averaging studies.

Our results include an estimate of the Hubble constant $H_0 = h$ 100 km s^{-1} Mpc^{-1} from the Tonry/Barris sample of 194 SNe Ia. Since the Tonry/Barris sample data used a fixed value of $h_{\rm fix} = 0.65$ (Tonry et al. 2003) in the derived distances, we divide their derived distances $H_0 d_L(z)$ by $h_{\rm fix}$ and marginalize over H_0 in our analysis. Our MCMC method yields smooth PDFs for all marginalized parameters. The errors on the estimated h in Tables 1 and 2 are statistical errors only, not including a much larger systematic error contributed by the intrinsic dispersion in SN Ia peak luminosity of $\sigma_m^{\rm int} \simeq 0.17$ mag (Hamuy et al. 1996). This implies a systematic uncertainty in h of 7.83%, or $\sigma_h^{\rm int} \simeq 0.05$ for the h-values tabulated in Tables 1 and 2. This yields an estimate for h that overlaps with those from Branch (1998) and Freedman et al. (2001) within 1 σ.

It is intriguing that the current SN Ia data, together with CMB and galaxy survey data, indicate that $\rho_X(z)$ varies with time at approximately 90% CL (see Fig. 3 and § 3.3). If the trend in $\rho_X(z)$ that we have found is confirmed by future observational data, it will have revolutionary implications for particle physics and cosmology. Since the uncertainty in $\rho_X(z)$ is large where there are few observed SNe Ia (see Fig. 3), we expect that a significant increase in the number of SNe Ia, obtained from dedicated deep SN Ia searches (Wang 2000a), will allow us to place robust and more stringent constraints on the time dependence of the dark energy density.

This work is supported in part by NSF CAREER grant AST 00-94335. We are grateful to David Branch and Michael Vogeley for helpful comments.

REFERENCES

Aguirre, A. N. 1999, ApJ, 512, L19
Alam, U., Sahni, V., Saini, T. D., & Starobinsky, A. A. 2003, preprint (astro-ph/0311364)
Albrecht, A., Burgess, C. P., Ravndal, F., & Skordis, C. 2002, Phys. Rev. D, 65, 123507
Barger, V., & Marfatia, D. 2001, Phys. Lett. B, 498, 67
Barris, B. J., et al. 2004, ApJ, 602, 571
Bean, R., & Melchiorri, A. 2002, Phys. Rev. D, 65, 041302
Bennett, C., et al. 2003, ApJS, 148, 1
Bernstein, G. M., & Jain, B. 2004, ApJ, 600, 17
Bond, J. R., Efstathiou, G., & Tegmark, M. 1997, MNRAS, 291, L33
Boyle, L. A., Caldwell, R. R., & Kamionkowski, M. 2002, Phys. Lett. B, 545, 17
Branch, D. 1998, ARA&A, 36, 17
Caldwell, R., Dave, R., & Steinhardt, P. 1998, Phys. Rev. Lett., 80, 1582
Carroll, S. M., Hoffman, M., & Trodden, M. 2003, Phys. Rev. D, 68, 023509

Choudhury, T. R., & Padmanabhan, T. 2003, preprint (astro-ph/0311622)
Daly, R. A., & Djorgovski, S. G. 2003, ApJ, 597, 9
Deffayet, C. 2001, Phys. Lett. B, 502, 199
Dodelson, S., Kaplinghat, M., & Stewart, E. 2000, Phys. Rev. Lett., 85, 5276
Drell, P. S., Loredo, T. J., & Wasserman, I. 2000, ApJ, 530, 593
Farrar, G. R., & Peebles, P. J. E. 2003, preprint (astro-ph/0307316)
Freedman, W. L., et al. 2001, ApJ, 553, 47
Freese, K., Adams, F. C., Frieman, J. A., & Mottola, E. 1987, Nucl. Phys. B, 287, 797
Freese, K., & Lewis, M. 2002, Phys. Lett. B, 540, 1
Frieman, J. A. 1997, Comments Astrophys., 18, 323
Frieman, J., Hill, J., Stebbins, A., & Waga, I. 1995, Phys. Rev. Lett., 75, 2077
Gerke, B. F., & Efstathiou, G. 2002, MNRAS, 335, 33
Griest, K. 2002, Phys. Rev. D, 66, 123501
Hamuy, M., et al. 1996, AJ, 112, 2408
Hannestad, S., & Mortsell, E. 2002, Phys. Rev. D, 66, 063508
Hawkins, E., et al. 2003, MNRAS, 346, 78
Holz, D. E., & Wald, R. M. 1998, Phys. Rev. D, 58, 063501
Hu, W. 2002, Phys. Rev. D, 66, 08351
Huterer, D., & Ma, C. 2004, ApJ, 600, L7
Huterer, D., & Turner, M. S. 2001, Phys. Rev. D, 64, 123527
Jimenez, R. 2003, NewA Rev., 47, 761
Kantowski, R., Vaughan, T., & Branch, D. 1995, ApJ, 447, 35
Knop, R. A., et al. 2003, ApJ, 598, 102
Kujat, J., Linn, A. M., Scherrer, R. J., & Weinberg, D. H. 2002, ApJ, 572, 1
Kuo, C. L., et al. 2004, ApJ, 600, 32
Lewis, A., & Bridle, S. 2002, Phys. Rev. D, 66, 103511
Majumdar, S., & Mohr, J. J. 2004, ApJ, in press (astro-ph/0305341)
Maor, I., Brustein, R., McMahon, J., & Steinhardt, P. J. 2002, Phys. Rev. D, 65, 123003
Maor, I., Brustein, R., & Steinhardt, P. J. 2001, Phys. Rev. Lett., 86, 6 (erratum 87, 049901)
Melchiorri, A., Mersini, L., Ödman, C. J., & Trodden, M. 2003, Phys. Rev. D, 68, 043509
Metcalf, R. B., & Silk, J. 1999, ApJ, 519, L1
Mukherjee, P., Banday, A. J., Riazuelo, A., Gorski, K. M., & Ratra, B. 2003, ApJ, 598, 767
Munshi, D., Porciani, C., & Wang, Y. 2004, MNRAS, in press (astro-ph/0302510)
Munshi, D., & Wang, Y. 2003, ApJ, 583, 566
Ödman, C. J., Melchiorri, A., Hobson, M. P., & Lasenby, A. N. 2002, Phys. Rev. D, 67, 083511
Padmanabhan, T. 2003, Phys. Rep., 380, 235
Pearson, T. J., et al. 2003, ApJ, 591, 556
Peebles, P. J. E., & Ratra, B. 1988, ApJ, 325, L17
———. 2003, Rev. Mod. Phys., 75, 559
Percival, W. J., et al. 2002, MNRAS, 337, 1068
Perlmutter, S., et al. 1999, ApJ, 517, 565
Phillips, M. M., 1993, ApJ, 413, L105
Podariu, S., & Ratra, B. 2001, ApJ, 563, 28
Press, W. H., Teukolsky, S. A., Vettering, W. T., & Flannery, B. P. 1994, Numerical Recipes (Cambridge: Cambridge Univ. Press)
Riess, A. G., Press, W. H., & Kirshner, R. P., 1995, ApJ, 438, L17
Riess, A. G., et al. 1998, AJ, 116, 1009
———. 1999, AJ, 118, 2675
Sahni, V., & Shtanov, Y. 2003, J. Cosmology Astroparticle Phys., 11, 14
Schulz, A. E., & White, M. 2001, Phys. Rev. D, 64, 043514
Seo, H., & Eisenstein, D. J. 2003, ApJ, 598, 720
Sereno, M. 2002, A&A, 393, 757
Spergel, D. N., et al. 2003, ApJS, 148, 175
Tegmark, M. 2002, Phys. Rev. D, 66, 103507
Tonry, J. L., et al. 2003, ApJ, 594, 1
Verde, L., et al. 2002, MNRAS, 335, 432
Viel, M., Matarrese, S., Theuns, T., Munshi, D., & Wang, Y. 2003, MNRAS, 340, L47
Wambsganss, J., Cen, R., Xu, G., & Ostriker, J. P. 1997, ApJ, 475, L81
Wang, Y. 1999, ApJ, 525, 651
———. 2000a, ApJ, 531, 676
———. 2000b, ApJ, 536, 531
Wang, Y., Freese, K., Gondolo, P., & Lewis, M. 2003, ApJ, 594, 25
Wang, Y., & Garnavich, P. 2001, ApJ, 552, 445
Wang, Y., Holz, D. E., & Munshi, D. 2002, ApJ, 572, L15
Wang, Y., & Lovelace, G. 2001, ApJ, 562, L115
Wasserman, I. 2002, Phys. Rev. D, 66, 123511
Weller, J., & Lewis, A.M. 2003, MNRAS, 346, 987
Zhu, Z., & Fujimoto, M. 2004, ApJ, 602, 12